Optimal Sampling Methodologies for High-rate Structural Twinning

Alexander B. Vereen*
Dept. of Mechanical Engineering
University of South Carolina
Columbia, USA
ORCID: 0000-0001-7175-7666

Emmanuel A. Ogunniyi*
Dept. of Mechanical Engineering
University of South Carolina
Columbia, USA
ORCID: 0000-0001-5456-5929

Austin R.J. Downey
Dept. of Mechanical Engineering
Dept. of Civil and Environmental Engineering
University of South Carolina
Columbia, USA
ORCID: 0000-0002-5524-2416

Erik Blasch
Air Force Research Laboratory
Arlington, USA
ORCID: 0000-0001-6894-6108

Jason D. Bakos
Dept. of Comp. Sci. and Engineering
University of South Carolina
Columbia, USA
ORCID: 0000-0002-0821-6258

Jacob Dodson
Air Force Research Laboratory
Arlington, USA
ORCID: 0000-0002-0852-5130

Abstract—In high-rate structural health monitoring, it is crucial to quickly and accurately assess the current state of a component under dynamic loads. State information is needed to make informed decisions about timely interventions to prevent damage and extend the structure's life. In previous studies, a dynamic reproduction of projectiles in ballistic environments (DROPBEAR) testbed was used to evaluate the accuracy of state estimation techniques through dynamic analysis. This paper extends previous research by incorporating the local eigenvalue modification procedure (LEMP) and data fusion techniques to create a more robust state estimate using optimal sampling methodologies. The process of estimating the state involves taking a measured frequency response of the structure, proposing frequency response profiles, and accepting the most similar profile as the new mean for the position estimate distribution. Utilizing LEMP allows for a faster approximation of the proposed model with linear time complexity, making it suitable for 2D or sequential damage cases. The current study focuses on two proposed sampling methodology refinements: distilling the selection of candidate test models from the position distribution and applying a Kalman filter after the distribution update to find the mean. Both refinements were effective in improving the position estimate and the structural state accuracy, as shown by the time response assurance criterion and the signal-to-noise ratio with up to 17% improvement. These two metrics demonstrate the benefits of incorporating data fusion techniques into the high-rate state identification process.

Index Terms—high-rate, structural health monitoring, data-fusion, modal, local eigenvalue modification procedure, real-time modeling

I. Introduction

In high-rate structural health monitoring (SHM) systems, real-time assessment of the state of the structure is crucial for enabling critical interventions. Such systems have potential to be used in various applications, such as aerospace, shock-prone systems, and civil infrastructure under high-rate loading. The system's state must be accurately determined promptly to allow control interventions to be made before failure. For aerospace structures, the target time is sub-millisecond for high rate and sub-100 nanoseconds for ultra-high rate [1].

Updating a physics-based model of the structure's state in real-time will create a digital twin of the structure [2]. A digital twin of a structure operating in high-rate environment needs to integrate ultra-low latency simulations with the structures' on-board health management system and all available historical and fleet data; to digitally mirror the condition of the physical twin. The concept of digital twinning for a structure operating in a high-rate environments was adopted from Glaessgen and Stargel's digital twin paradigm for next-generation aircraft [3]. Additionally, Digital twins, using first principle models, (such as the dynamic data driven applications systems paradigm), and generative AI have shown promise in data fusion systems as discussed by Paul et al. [4] and Lei et al. [5]

A digital twin of the structure enables damage evolution models informed by high-rate SHM; thereby enabling unprecedented levels of safety and reliability. The implementation of a digital twin in high-rate SHM is necessary to limit the search space and avoid testing all candidate models with some arbitrary amount of damage characteristics, which grows exponentially with the amount of considered data. In related work on discrete dynamic systems, Ganguli and Adhikari [6] developed a digital twin framework of a damped dynamic system that can propose frequency profiles that may be non-unique but identifiable; based on the previous belief of the system state.

Sensor and information fusion techniques play a key role in enabling computationally efficient digital twinning of structures discussed by Blasch et al. [7] and Wu et al. [8]. Previous

This work is partly supported by the National Science Foundation Grant numbers 1850012, 1956071, and 2237696 as well as the Air Force Research Laboratory. The support of these agencies is gratefully acknowledged. Any opinions, findings, conclusions, or recommendations expressed in this material are those of the authors, and they do not necessarily reflect the views of the National Science Foundation or the United States Air Force.

work on information fusion for structural model updating includes that by Zhu et al. where a multi-rate Kalman filtering approach was used to merge measured strain and acceleration data to achieve low-noise displacement measurements in super tall structures [9]. Likewise, Ren et al. used multi-rate Kalman filtering with stochastic subspace identification to calculate the strain mode before fusing strain-derived displacement and acceleration data to reconstruct the structure's dynamic displacement [10]. In a direct-to-model approach, Mooij et al. utilized an inverse finite element method to determine structural deformation from a reduced number of distributed sensors on cantilever beams [11].

This study utilizes the Dynamic Reproduction of Projectiles in Ballistic Environments for Advanced Research (DROPBEAR) testbed [12] to generate controlled experimental data of a structure undergoing structural degradation. The testbed consists of a cantilever beam with a rolling pinned boundary condition along its length, which is controlled in real-time by a linear actuator. The system's state is inferred from the accelerometer mounted on the end of the cantilever beam. In previous studies using the DROPBEAR testbed, the state estimation problem was tackled by comparing the similarity in frequency response between the proposed system state and the modeled system response [13]. The beam was modeled using a one-dimensional finite element formulation with Euler-Bernoulli elements. Solving for the eigenvalues of the DROPBEAR system provides an estimate of the beam's frequency response under free excitation. However, the eigenvalue solution step requires $O(N^2)$ time, where N is proportional to the number of nodes in the discretized beam.

The Local Eigenvalue Modification Procedure (LEMP) has been previously shown to reformulate the eigenvalue estimation step as an $O(N)$ task [14, 15]. Instead of solving for eigenvalues, LEMP estimates changes in eigenvalues based on a singular change in the stiffness or mass matrices describing the system. LEMP allows for the estimation of eigenvalues as an update to two previously solved reference states, with the limitation that a singular modification must cause the change to the system. For example, the reference state can be modeled as a free one-dimensional cantilever beam, and the singular modification can be modeled as a significant increase in the stiffness matrix localized to the hypothesized pin location.

Although solving for all possible states and using a lookup table for eigenvalue solutions is more effective than using LEMP for singular modifications in one-dimensional problem spaces, LEMP holds promise for applications involving modifications to two-dimensional systems (e.g., thin plates) or multiple sequential modifications. For such a 2D problem, the complexities introduced by the dimensionality make the required size of a lookup table entirely impractical for applications where all pre-calculated solutions are required.

This study investigates the use of linear quadratic estimation (LQE), also known as Kalman filtering (KF), in combination with optimal sampling methodologies to enable high-rate structural twinning with great accuracy and reduced computational load when compared to previously investigated techniques [15], [16]. The model updating technique is explained in detail by Downey et al. [17] and, in brief, uses an online error minimization model updating approach that seeks to find the optimal finite element model (FEM) boundary conditions by minimizing the error between the structure's and the model's response, where the finite element model's response is calculated in real-time using LEMP.

The four sampling techniques investigated in this work are 1) Bayesian inference, 2) likelihood ratio test, 3) Metropolis-Hasting algorithm, and 4) Gibbs sampling. Each sampling method is investigated with and without a KF formulation to identify the optimal finite element analysis (FEA) model boundary conditions by updating the sample distribution. By minimizing the number of sample candidates that need to be computed, the proposed work reduces the required computational resources, enabling the future deployment of high-rate structural twinning at the edge. The contributions of this work are twofold, 1) the LEMP model updating approach is extended with the use of a KF for real-time sample distribution updating, and 2) four sampling methodologies are investigated in combination with the KF for high-rate model updating.

II. Background

This section describes the relevant background covering the DROPBEAR testbed and LEMP.

A. Testbed

In this work, a one-dimensional FEA formulation of the DROPBEAR, shown in Figure 1, is used to study the potential benefits of data fusion techniques in structural health monitoring applications [12]. The DROPBEAR consists of a cantilever beam with an accelerometer mounted to its end, and a rolling pin condition is used to excite the structure and change the system's state. As a result, the structure's frequency changes in a predictable way in response to the change in boundary conditions. Several methods are proposed to obtain the roller's location (e.g., state) from a distribution of candidate system states. Finally, to corroborate the ground truth of the estimation, a magnetic position sensor is used to obtain the roller's true roller position or state. The dataset used in this work is available through an open-source dataset [18].

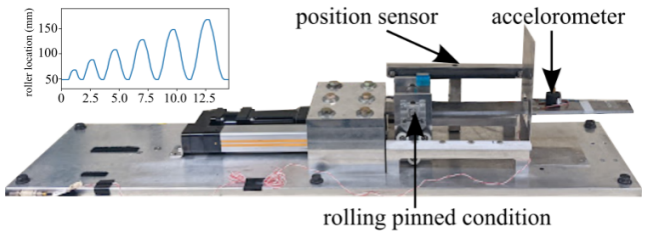

Fig. 1. The experimental Dynamic Reproduction of Projectiles in Ballistic Environments for Advanced Research (DROPBEAR) testbed used in this work to generate the open-source dataset [18].

B. LEMP

The local eigenvalue modification procedure (LEMP) was introduced to simplify Structural Dynamic Modification

(SDM) calculations, especially when only one change is made to the system. SDM is a method for identifying changes made to a system's physical parameters, such as mass, stiffness, or damping, by monitoring its dynamic response [14].

LEMP simplifies the state's calculations by truncating the number of independent single-degree-of-freedom systems to include only the most significant modes of interest. The generalized eigenvalue equation is then reduced to a set of second-order equations whose roots are determined by the system's initial frequencies, which reduces the number and complexity of equations required to compute the structure's state [19]. The LEMP process leads to shorter computation times as the dynamic response of the structure can be solved for without computing the generalized eigenvalue problem. However, to implement LEMP, it is important to make assumptions about the system's current state, such as the geometry, material, and boundary conditions. The initial guess about the system's state can be any arbitrary singular structural modification from that assumption. It is also noted that LEMP will converge to the closest representation of the actual state.

Prior work by Ogunniyi et al. [16] developed a real-time computing module to enable the use of LEMP in high-rate model updating with a stringent latency constraint of 1 ms. The real-time computing module uses a divide-and-conquer approach to iteratively solve the roots of the secular equations, leading to faster root convergence. Using the divide-and-conquer approach result, the LEMP algorithm provides a more efficient and streamlined approach to calculating the altered state of a system compared to traditional SDM methods.

III. Methodology

The LEMP model updating methodology is presented in Figure 2. It extends the previously proposed and investigated error minimization model updating technique [15] with the KF to obtain an optimal selection of potential candidate models and is investigated alongside four different modifications mathematically robust sampling. The extended aspects of the error minimization model updating technique are denoted with the dashed-red box in Figure 2. The remainder of this Section discusses the details of the extended error minimization model updating technique.

Key metrics of the signal-to-noise ratio (SNR_{dB}) and the time response assurance criterion (TRAC) in Eq. (1, 2), are used to quantify the error in state estimation, where t_m and t_e are time traces of the measured and estimated data, respectively. TRAC is a method that quantifies between zero and one the similarity between time traces by comparing the numerical error and time delay of each estimation [20]. A TRAC score of 1 means perfect timing alignment, while a score of 0 means no temporal correlation between signals.

$$SNR_{dB} = 10 \log_{10} \frac{P_{signal}}{P_{noise}} \quad (1)$$

$$TRAC = \frac{[\{t_m\}^T\{t_e\}]^2}{[\{t_m\}^T\{t_m\}][\{t_e\}^T\{t_e\}]} \quad (2)$$

A. Kalman Filter

The KF is a method for estimating the unknown state of a system based on observations of its dynamic behavior. In tracking applications, several models can be used. However, the constant velocity model is particularly useful when it is assumed that the rate of change of the system is constant between measurement samples, especially when the sampling rate is high [21]. Furthermore, a KF model offers several advantages, such as linearity and simplicity in implementation. In the present case, where the hidden state models the roller's position along the beam, and the measurement is obtained using the LEMP-enabled structural health monitoring scheme (as outlined in Figure 2), where utilizing the KF appears to be an ideal solution for isolating and refining the estimation of the roller's true position.

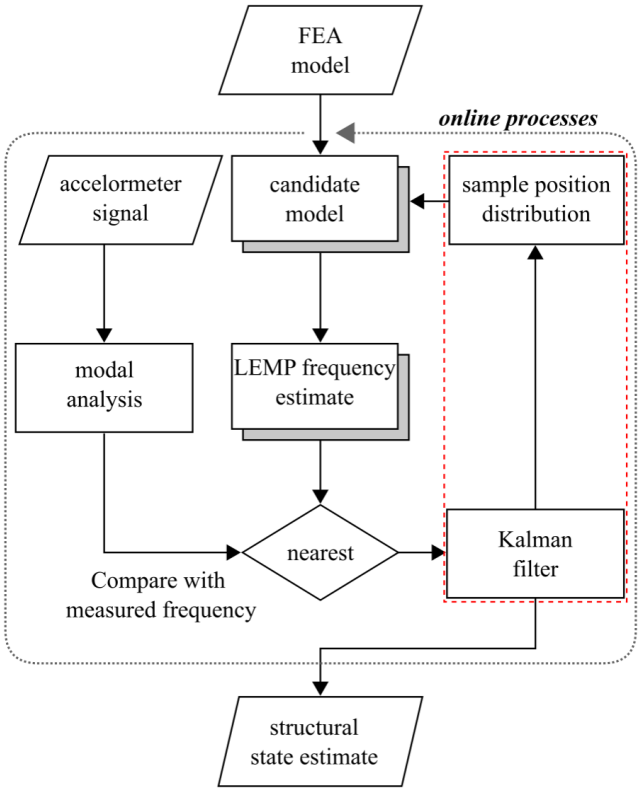

Fig. 2. Flowchart of the LEMP process used in this work to enable real-time structural state estimation where the red box denotes the extension to the previously proposed LEMP model-updating approach.

In terms of the state equation modeling for the KF, the measured variable for the DROPBEAR application is the noisy estimate of the current roller y_k, using the time step subscript k for this discrete model, that is used to ascertain the true hidden state of the roller x_k. In the state space representation, x_k is the expected transition from the previous state to the current time step, linearly proportional to the transition matrix A_k. The measurement of each step is described as a linear relation between the measurement transition matrix C_k and the output y_k from state x_k from the measurement z_k. The process is modeled as a linear Gaussian process where the noise (w_p

, w_r) is additive, and the distributions are independently and identically distributed.

$$\begin{aligned} x_k &= A_k x_{k-1} + w_p \\ y_k &= C_k x_k + w_r \end{aligned} \tag{3}$$

The KF is a Bayesian filter that starts by setting a priori belief about the state at the current time step k and then adjusts this belief based on the measurement, considering its likelihood given the prior [22]. Eqs. (4, 5) show the calculation of the a priori estimate of the state and the estimate of the covariance $\hat{P}$, where $A_k \hat{P}_{s,k-1} A_k^T$ denotes the expected noise propagated in the model from the prior time step and Q_k quantifies the estimated state covariance, of the distribution around that state [22, 23] where the hat denotes an estimated value. All estimations made by the KF prior to the measurement update are denoted by the subscript a, as in antecedent, indicating that they are made before the measurement update. The subscript s, as in subsequent for this notation, denotes that they are made after the measurement update.

- a priori estimate

$$\hat{x}_{a,k} = A_k \hat{x}_{s,k-1} \tag{4}$$

$$\hat{P}_{a,k} = A_k \hat{P}_{s,k-1} A_k^T + Q_k \tag{5}$$

- measurement innovation and update

$$\tilde{y}_k = z_k - C_k \hat{x}_{a,k} \tag{6}$$

$$S_k = C_k \hat{P}_{a,k} C_k^T + R_k \tag{7}$$

$$\epsilon_k = \tilde{y}_k^T (S_k) \tilde{y}_k \tag{8}$$

$$L_k = \hat{P}_{a,k} C_k^T S_k^{-1} \tag{9}$$

The measurement and apriori expected measurement, z_k and $C_k \hat{x}_{a,k}$ respectively, are then incorporated by computing the innovation $\tilde{y}_k$ shown in Eq. (6). The innovation covariance S_k, or the believability of the innovation, is calculated as the sum of the noise covariance in the innovation R_k and the predicted innovation covariance $C_k \hat{P}_{a,k} C^T$ as shown in Eq. (7). The innovation values are used to calculate the Kalman gain L_k and the Normalized Innovation Squared (NIS) metric ϵ_k, as shown in Eqs. (8, 9). The NIS is a chi-square distributed metric that can be used to assess whether the residual, as measured by the innovation, is consistent with the innovation covariance. Suppose the NIS value exceeds an acceptable interval [24]. In that case, the measurement can be rejected as an outlier, which is useful in systems where inputs may be faulty, or outliers may be present in the noise [25]. The NIS is particularly important for the tracking problem, as the noise covariance of the innovation should enable us to automatically enable rejection of large changes in the measured position, which may result from similarities in the first mode response across the structures.

- a posteriori state estimate

$$\hat{x}_{s,k} = \hat{x}_{a,k} + L_k \tilde{y}_k \tag{10}$$

$$\hat{P}_{s,k} = (I - L_k C_k) \hat{P}_{a,k} \tag{11}$$

The a posteriori state estimate is obtained by combining the a priori estimate and the measurement innovation, weighted by the Kalman gain. If the NIS value is rejected, the Kalman gain is set to zero, thus rejecting the measurement innovation, and the a priori estimate is used as the best estimate [22, 23]. On the other hand, suppose the NIS falls within the acceptable interval. In that case, the a posteriori estimate of the state and covariance, $\hat{x}_{s,k}$ and $\hat{P}_{s,k}$, respectively, are considered the most likely state of the system and are used for further processing. In eq 11, I is the identity matrix.

B. Sampling

Sampling is used to select an optimal point along the length of the DROPBEAR beam. This work investigates four sampling methods for obtaining an appropriate roller location on which LEMP is applied for state estimation. This is in contrast to the authors' prior method of randomly selecting a point from a Gaussian distribution to apply LEMP. The four sampling methods used are shown in Figure 3.

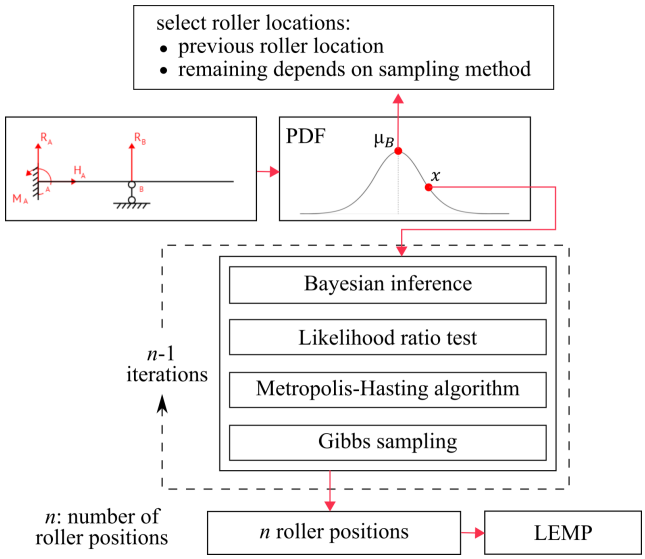

Fig. 3. Sampling process used for selecting roller locations on the DROPBEAR testbed structure where only one of the four listed sampling methods is used at a time.

1) Bayesian Inference: Three points are selected by sampling from a normal distribution centered on the previous roller position. The first point is assumed to be the previous mean μ_B without damage. A random point (x) is then chosen above the mean, and the likelihood functions for this point (x) are calculated using Eqs. (12, 13) for the two previous distributions, where σ is the standard deviation. Here, the distribution prior to "B" is represented by "A" and "B" represents the previous distribution to determine the estimate (E) given the right (R) and left (L) movements.

$$P(E|R) = \frac{1}{\sqrt{2\pi\sigma^2}} \exp\frac{-1}{2}\frac{(x-\mu_B)^2}{2\sigma^2} \quad (12)$$

$$P(E|L) = \frac{1}{\sqrt{2\pi\sigma^2}} \exp\frac{-1}{2}\frac{(x-\mu_A)^2}{2\sigma^2} \quad (13)$$

The direction of the roller's last movement can be determined by comparing μ_B to μ_A. If μ_B was greater than μ_A, the roller moved to the right. The roller moved to the left if μ_A is greater than μ_B. The likelihood function is used in Bayes' theorem to update the probability of a hypothesis given new data. The output of Eq. (14) represents the updated distribution for the roller's location after considering previous location selections and likelihoods [26]. If the probability of the roller moving to the right $P(R|E)$ is greater than 0.5, the two remaining sample locations are chosen above the previous mean value. If the probability of the roller moving to the left is less than 0.5, the two remaining sample locations are chosen below the previous mean value. If $P(R|E) = 0.5$, the remaining two sample locations are chosen randomly.

$$P(R|E) = \frac{P(R)P(E|R)}{P(R)P(E|R) + P(L)P(E|L)} \quad (14)$$

2) Likelihood Ratio Test: The likelihood ratio test (LRT) is a statistical test used to compare the fit of two different models to a given data set. It is based on the ratio of the maximum likelihoods (ML) of the two models and is used to determine which model best fits the data.

Given a set of data and two models, M_1 and M_2, the likelihood ratio test statistic is given by:

$$LRT = 2 \times (\ln(L(M_1)) - \ln(L(M_2))) \quad (15)$$

where $L(M_1)$ and $L(M_2)$ are the maximum likelihoods of the two models, respectively. Under the null hypothesis that M_1 is the true model, the LRT statistic follows a chi-squared distribution with the degrees of freedom equal to the difference in the number of parameters between the two models.

Two models for the data are defined to use the LRT to select a roller location from a uniform distribution. The first model, M_1, is a uniform distribution over the range (a, b), and the second model, M_2, is a uniform distribution over the range (c, d) where $c > a$ and $d > b$. The maximum likelihoods of the two models are then calculated using the data. Suppose $L(M_1) > L(M_2)$, the null hypothesis that M_1 is the true model is rejected, and M_2 is accepted as the true model. This means that the location is selected from the range (c, d), whereas if $L(M_1) < L(M_2)$, the location is selected from the range (a, b) [27].

3) Metropolis-Hasting Algorithm: The Metropolis-Hastings Algorithm is a Markov Chain Monte Carlo (MCMC) technique that generates samples from a target distribution by proposing new states and accepting or rejecting them based on the target distribution. The MH algorithm is used to select a roller location from a uniform distribution on a beam.

The Metropolis-Hastings Algorithm requires defining a proposal distribution, $q(x'|x)$ is the conditional probability of proposing a state x' given x. Conversely, $q(x|x')$ denotes the probability of proposing a state x given x'. In this case, a simple proposal distribution is a normal distribution with mean x and fixed standard deviation over the range (a, b). The acceptance probability (α) of a candidate state x' is given by the formula:

$$\alpha = \min\left(1, \frac{p(x') \times q(x|x')}{p(x) \times q(x'|x)}\right) \quad (16)$$

where $p(x)$ is the target distribution. Here α is calculated as the ratio of the target distribution at the candidate state to the current state [28]. The process for the Metropolis-Hastings Algorithm begins by initializing the chain with an initial value of x. In each iteration, a candidate state, x', is generated from the proposal distribution, $q(x'|x)$. The candidate state is then accepted with probability α. If the candidate state is accepted, the chain is updated to the new state, x'. Otherwise, the chain remains in the current state, x. The process is repeated for a specified number of iterations, and the resulting samples are stored in a list.

4) Gibbs Sampling: The Gibbs sampling algorithm is a Markov Chain Monte Carlo (MCMC) method used to generate samples from a multivariate distribution. It operates by iteratively sampling each variable from its full-conditional distribution, given the current values of all other variables.

To implement Gibbs sampling, the target distribution, $p(x)$, is decomposed into a set of full-conditional distributions, one for each variable. In the case of a uniform distribution over (a, b), the full-conditional for the variable x is simply a uniform distribution over the same range (a, b). The full-conditional for x is represented by the following probability density function (PDF) [29]:

$$p(x|x_1, \ldots, x_n) = \frac{1}{b-a} \text{ for } a \le x \le b \quad (17)$$

where $x_1, x_2, \ldots, x_n$ are the current values of all other variables. To generate a roller location from the target distribution using Gibbs sampling, the chain is initialized with an initial value of x. Then the chain is updated iteratively by drawing new samples from the full-conditional distribution for x, given the current value of x. The locations generated by the chain are stored in a list, and a random point is selected from the list of locations.

C. Comparison Criteria

Real-time updating of the model can be done in two stages: 1) determining the analytical frequency at specific roller positions, and 2) selecting the best estimation to depict the current system state by using comparison techniques. This study's analytical solutions for system states are obtained using LEMP under four sampling methods.

The analytical solutions are utilized to approximate system states through error minimization, referred to as nearest neighbor, and bounded regression. Both methods use three comparison points. The nearest neighbor method compares the actual (measured) frequency with the frequency at the three test points and selects the location that minimizes the absolute

error. The bounded regression method is taken from Hong et al. [30], where the linear model by the least-squares method is represented by Eq. (18) [31].

$$\begin{matrix} a \\ b \end{matrix} = (X^T X)^{-1} X^T Y \tag{18}$$

Three locations have been selected for analysis when comparing the frequency of roller locations. Locations X and Y are defined as follows, where x_n are sample locations along the beam:

$$X = \begin{bmatrix} x_1 & 1 \\ x_2 & 1 \\ x_3 & 1 \end{bmatrix} \tag{19}$$

$$Y = \begin{bmatrix} \omega_1 - \omega_{true} \\ \omega_2 - \omega_{true} \\ \omega_3 - \omega_{true} \end{bmatrix} \tag{20}$$

The regression model's parameters a and b represent the slope and y-intercept, respectively. The difference between the estimated ω and the true ω_{true} can be represented by the linear equation $\omega - \omega_{true} = ax + b$. The estimated ω will equal the true ω when the input variable x equals $-b/a$. However, due to limitations in the sample data used for the regression, the estimated roller location is restricted to the range between the minimum and maximum comparison locations.

IV. Results

The results presented here discuss the use of sampling methodologies in data fusion and analysis for state estimation of high-rate dynamic systems.

A. LEMP Estimate

Figure 4 displays the roller state estimation described previously, where the roller locations are sampled randomly from a Gaussian distribution and input into the LEMP algorithm [16]. The roller is assumed to be continuously moving to the right, signifying a system deterioration over time (i.e..., progressive damage). As a result, roller locations are randomly selected above the previous mean (current roller position). The initial roller location on the distribution before applying the sampling techniques is selected using Eq. (21), where r represents a random number, σ is the standard deviation, and B is the current roller location.

$$\text{abs}(r \times \sigma + B) \tag{21}$$

The estimation was compared using both the nearest neighbor and least square regression comparison criteria. As shown in Figure 4, many outliers exist in the estimated roller position when using a 21-node beam model. However, increasing the number of nodes to 101 improves the estimation result, as seen in the same Figure 4. Although increasing the number of nodes improves the accuracy, it also increases the computational time. The nearest neighbor considers the closest to the true value as the current roller position, hence the reason for the steps or square edges shown in the estimate of the roller location in Figure 4. The regression uses the least square regression formula to calculate the roller position using the output from LEMP. Of the two metrics used to evaluate the estimation accuracy, the least square regression criteria performed better than the nearest neighbor. As a result, only the least square regression will be used to introduce sampling techniques, as the goal is to achieve optimal estimation.

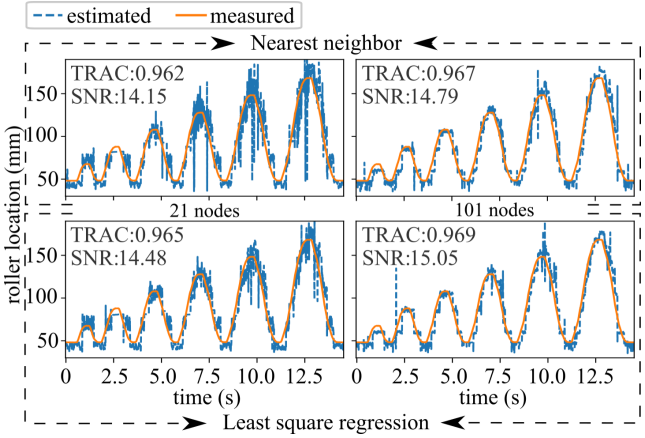

Fig. 4. Estimation results obtained using LEMP with a 21-node and 101-node model of the beam and the previously investigated Gaussian sampling technique without the use of a KF; termed the "base state".

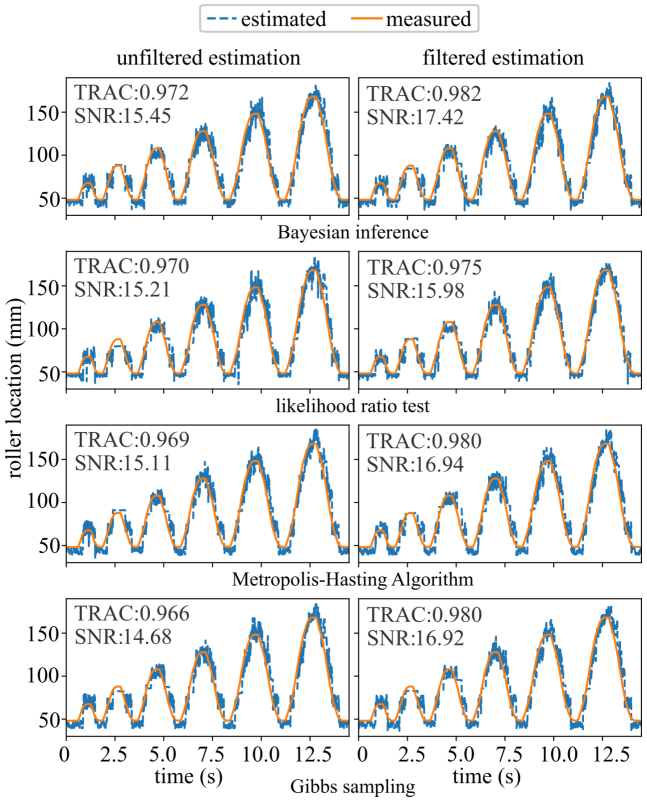

Fig. 5. State estimation results on a 21-node model of the beam with LEMP in the filtered and unfiltered configuration where Bayes inference, Likelihood ratio test, Metropolis-Hasting Algorithm, and Gibbs sampling are used to sample roller location.

B. Improved LEMP Estimate

A state estimation using LEMP was performed by pairing four sampling methods with a KF to track the roller positions on a beam. Two approaches were taken. First, an unfiltered estimation, where the roller positions were sampled using the four methods and fed directly into the LEMP algorithm without KF refinement. Second, a filtered estimation, where the sampled roller locations were optimized using the KF, and then the LEMP algorithm was used to determine the new position frequency. Figure 5 shows the estimation results using a 21-node beam model to estimate the roller position. In the unfiltered configuration, the Bayesian sampling showed the best results with a TRAC of 0.972 and a signal-to-noise ratio of 15.456. All sampling methods produced improved results compared to results without sampling on the 21-node beam model (Figure 4). Table I displays the improvement in estimation results, measured as a percentage, using the KF alongside each sampling technique. The Table I result is calculated by comparing results from Figure 5 and Figure 7 to results in Figure 4.

An extended view of the estimation result is shown in Figure 6. The Figure 6 shows how sampling improves the state estimation of the roller position on the beam. Fig-ure 6(a) is the generic LEMP estimate. Figure 6(b) displays the improved LEMP estimate that uses Bayesian sampling to identify suitable roller positions. Finally, Figure 6(c) shows the LEMP estimate refined using the KF after Bayesian search space sampling. The results showed that the estimated position becomes better aligned with the true measured position from Figure 6(a)-(c), and the TRAC and SNR values also increase accordingly.

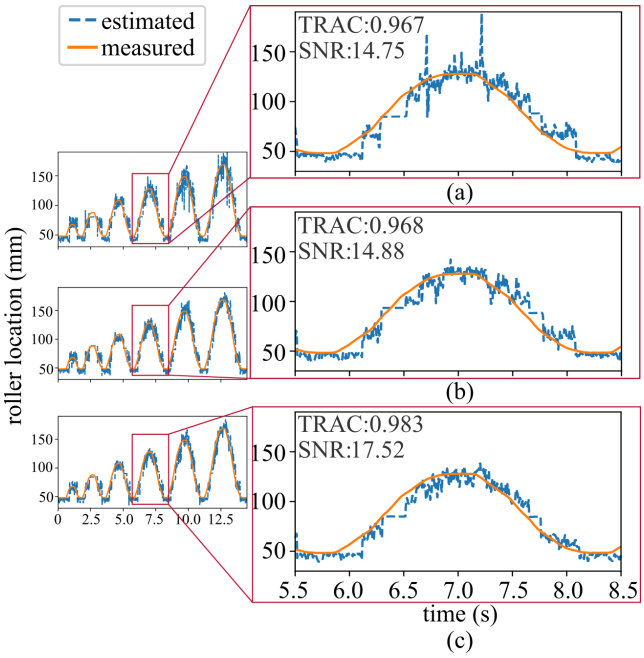

Fig. 6. Roller position estimation using a 21-node beam model for: (a) LEMP estimate without sampling methodology and KF application, and; (b) LEMP estimate where roller positions are sampled using Bayesian search space; (c) improved LEMP estimate where roller positions are sampled using the Bayesian search space and also filtered with the KF.

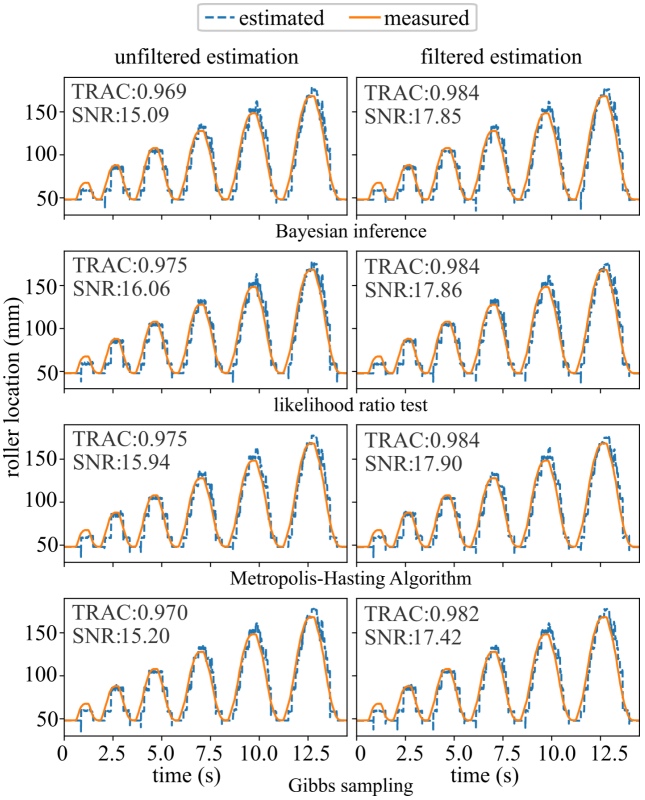

Fig. 7. State estimation results on 101-noded beam with LEMP in the filtered and unfiltered configuration where Bayes inference, Likelihood ratio test, Metropolis-Hasting Algorithm, and Gibbs sampling are used to sample roller location.

While the KF improved the estimation results, further improvement can be made by increasing the number of nodes used to model the beam. The sampled roller positions will be closer to the true values with more nodes. Figure 7 shows the estimation results with a 101-node beam model, which show a significant improvement in the estimated roller position. The unfiltered configuration was compared to the filtered configuration for this beam model. For each sampling method, the results were better with the use of the KF to refine the mean of the distribution. The improvement was observed in both the 21-node and 101-node models, where the likelihood ratio test (LRT) alongside the KF showed the best improvement.

TABLE I
AVERAGE PERCENTAGE IMPROVEMENT IN SNR_{dB} COMPARED TO ESTIMATION WITHOUT SAMPLING AND KF AT 21 AND 101 NODES FOR THREE PARTICLE MODELS OVER 100 TRIALS.

	SNR_{dB} improvement			
	21 nodes		101 nodes	
sampling method	unfiltered	filtered	unfiltered	filtered
Bayesian inference	3.03%	15.86%	0.95%	13.93%
likelihood ratio test	5.30%	17.18%	2.64%	14.69%
Metropolis-Hasting Algorithm	0.87%	13.27%	-0.18%	13.47%
Gibbs sampling	0.72%	12.53%	0.33%	14.28%
Gaussian sampling	base case	13.14%	base case	14.69%

V. Conclusions

The study demonstrated the benefits of using the KF in the model updating process to improve accuracy and maintain timely updates. The traditional model updating method involved finding the closest frequency match to the observed frequencies of the live structure, but this was improved upon by introducing the extended error minimization approach. In this new method, the closest frequency estimate was treated as a noisy measurement for a KF, which was used to track changes in the boundary conditions. The refined state estimate produced by the KF was then used to generate new models for the next time step. The study found that the likelihood ratio test alongside the linear KF effectively produced accurate results, with an 17% increase in accuracy for a 21-node model of the considered structure. The study also highlighted the importance of filtering outliers, as demonstrated by using the Normalized Innovation Squared (NIS) metric. This study successfully improved accuracy over traditional model updating methods, especially for lightweight models with low node counts on all the methodologies tested.

In future studies, the methodology would be expanded to include two-dimensional analysis and sequential damage cases, emphasizing the need for intelligent model selection and outlier filtering.

The authors would like to declare the views and conclusions contained herein are those of the author and should not be interpreted as necessarily representing the official policies or endorsements, either expressed or implied, of the Authors Universities, Industries, or the U.S. Government.

References

[1] Jacob Dodson, Austin Downey, Simon Laflamme, Michael D. Todd, Adriane G. Moura, Yang Wang, Zhu Mao, Peter Avitabile, and Erik Blasch. High-rate structural health monitoring and prognostics: An overview. In Data Science in Engineering, Volume 9, pages 213–217. Springer International Publishing, oct 2021.

[2] Frederica Darema Sai Ravela Alex J. Aved, Erik P. Blasch, editor. Handbook of Dynamic Data Driven Applications Systems. Springer International Publishing, May 2022.

[3] Edward Glaessgen and David Stargel. The digital twin paradigm for future NASA and u.s. air force vehicles. In 53rd AIAA/ASME/ASCE/AHS/ASC structures, structural dynamics and materials conference 20th AIAA/ASME/AHS adaptive structures conference 14th AIAA. American Institute of Aeronautics and Astronautics, apr 2012.

[4] Saswata Paul, Elkin Cruz, Airin Dutta, Ankita Bhaumik, Erik Blasch, Gul Agha, Stacy Patterson, Fotis Kopsaftopoulos, and Carlos Varela. Formal verification of safety-critical aerospace systems. IEEE Aerospace and Electronic Systems Magazine, pages 1–14, 2023.

[5] Xiaoming Lei, Limin Sun, and Ye Xia. Lost data reconstruction for structural health monitoring using deep convolutional generative adversarial networks. Structural Health Monitoring, 20(4):2069–2087, oct 2020.

[6] Ranjan Ganguli and Sondipon Adhikari. The digital twin of discrete dynamic systems: Initial approaches and future challenges. Applied Mathematical Modelling, 77:1110–1128, jan 2020.

[7] Erik Blasch, Jaimie Tiley, Daniel Sparkman, Sean Donegan, and Matthew Cherry. Data fusion methods for materials awareness. In Lynne L. Grewe, Erik P. Blasch, and Ivan Kadar, editors, Signal Processing, Sensor/Information Fusion, and Target Recognition XXIX. SPIE.

[8] Rih-Teng Wu and Mohammad Reza Jahanshahi. Data fusion approaches for structural health monitoring and system identification: Past, present, and future. Structural Health Monitoring, 19(2):552–586, sep 2018.

[9] Hongping Zhu, Ke Gao, Yong Xia, Fei Gao, Shun Weng, Yuan Sun, and Qin Hu. Multi-rate data fusion for dynamic displacement measurement of beam-like supertall structures using acceleration and strain sensors. Structural Health Monitoring, 19(2):520–536, jun 2019.

[10] Liang Ren, Qing Zhang, and Xing Fu. Theoretical derivation and experimental investigation of dynamic displacement reconstruction based on data fusion for beam structures. Scientific Reports, 12(1), nov 2022.

[11] Cornelis De Mooij, Marcias Martinez, and Rinze Benedictus. Sensor fusion for shape sensing: Theory and numerical results. 2016.

[12] Matthew Nelson, Simon Laflamme, Chao Hu, Adriane G Moura, Jonathan Hong, Austin Downey, Peter Lander, Yang Wang, Erik Blasch, and Jacob Dodson. Generated datasets from dynamic reproduction of projectiles in ballistic environments for advanced research (DROPBEAR) testbed. IOP SciNotes, 3(4):044401, nov 2022.

[13] Austin Downey, Jonathan Hong, Jacob Dodson, Michael Carroll, and James Scheppegrell. Millisecond model updating for structures experiencing unmodeled high-rate dynamic events. Mechanical Systems and Signal Processing, 138:106551, apr 2020.

[14] Peter Avitabile. Twenty years of structural dynamic modification-a review. Sound and Vibration, 37(1):14–27, 2003.

[15] Claire Rae Drnek. Local eigenvalue modification procedure for real-time model updating of structures experiencing high-rate dynamic events. Master's thesis, University of South Carolina, 2020.

[16] Emmanuel Ogunniyi, Austin R. J. Downey, and Jason Bakos. Development of a real-time solver for the local eigenvalue modification procedure. In Daniele Zonta, Zhongqing Su, and Branko Glisic, editors, Sensors and Smart Structures Technologies for Civil, Mechanical, and Aerospace Systems 2022. SPIE, apr 2022.

[17] Austin Downey, Jonathan Hong, Jacob Dodson, Michael Carroll, and James Scheppegrell. Millisecond model updating for structures experiencing unmodeled high-rate dynamic events. Mechanical Systems and Signal Processing, 138:106551, apr 2020.

[18] Austin Downey, Jonathan Hong, Jacob Dodson, Michael Carroll, and James Scheppegrell. Dataset-2-dropbear-acceleration-vs-roller-displacement, April 2020.

[19] J. T. Weissenburger. Effect of local modifications on the vibration characteristics of linear systems. Journal of Applied Mechanics, 35(2):327–332, jun 1968.

[20] Peter Avitabile and Pawan Pingle. Prediction of full field dynamic strain from limited sets of measured data. Shock and Vibration, 19(5):765–785, 2012.

[21] Gabriel F. Basso, Thulio Guilherme Silva De Amorim, Alisson V. Brito, and Tiago P. Nascimento. Kalman filter with dynamical setting of optimal process noise covariance. IEEE Access, 5:8385–8393, 2017.

[22] R. E. Kalman. A new approach to linear filtering and prediction problems. Journal of Basic Engineering, 82(1):35–45, mar 1960.

[23] Greg Welch, Gary Bishop, et al. An introduction to the kalman filter. 1995.

[24] Zhaozhong Chen, Christoffer Heckman, Simon Julier, and Nisar Ahmed. Weak in the nees?: Auto-tuning kalman filters with bayesian optimization, 2018.

[25] Shigeru Imai, Erik Blasch, Alessandro Galli, Wennan Zhu, Frederick Lee, and Carlos A. Varela. Airplane flight safety using error-tolerant data stream processing. IEEE Aerospace and Electronic Systems Magazine, 32(4):4–17, apr 2017.

[26] Ming Li and William Q. Meeker. Application of bayesian methods in reliability data analyses. Journal of Quality Technology, 46(1):1–23, jan 2014.

[27] John A. Rice. Mathematical Statistics and Data Analysis (with CD Data Sets) (Duxbury Advanced). Duxbury Press, 2006.

[28] Woody K. Hastings. Monte carlo sampling methods using markov chains and their applications. Biometrika, 57(1):97–109, apr 1970.

[29] Dipak K. Dey, Sujit K. Ghosh, and Bani K. Mallick, editors. Generalized Linear Models. CRC Press, may 2000.

[30] Seong Hyeon Hong, Claire Drnek, Austin Downey, Yi Wang, and Jacob Dodson. Real-time model updating algorithm for structures experiencing high-rate dynamic events. In ASME 2020 Conference on Smart Materials, Adaptive Structures and Intelligent Systems. American Society of Mechanical Engineers, sep 2020.

[31] Trevor Hastie, Robert Tibshirani, Jerome H Friedman, and Jerome H Friedman. The elements of statistical learning: data mining, inference, and prediction, volume 2. Springer, 2009.